FACULDADE DE ENGENHARIA DA UNIVERSIDADE DO PORTO

Relative acoustic localization with USBL (Ultra Short BaseLine)

Paula Alexandra Agra Graça

WORKING VERSION

Master in Electrical and Computers Engineering

Supervisor: José Carlos Alves

Co-supervisor: Bruno Ferreira

August 27, 2020

© Paula Alexandra Agra Graça, 2020

Resumo

Dispositivos robóticos programáveis como *Autonomous Underwater Vehicles* (AUVs) são excelentes meios para exploração subaquática, já que são capazes de executar missões de longa duração com variadas possibilidades de aplicação e objetivos. Neste sentido, o conceito de mula AUV surgiu como mecanismo útil que periodicamente recolhe dados dos AUVs em missão. Para que tal seja possível, é necessário implementar um sistema de localização e posicionamento robusto que permite aos AUVs encontrarem outros veículos de forma a aproximarem-se deles eficientemente.

A presente dissertação foca-se na implementação de um sistema que estima a posição relativa entre AUVs através do método *Ultra-Short Baseline* (USBL). Esta técnica baseia-se na determinação da diferença de fases entre sinais recebidos por um vetor de hidrofones.

Após a implementação e validação do sistema referido, este foi integrado num mecanismo existente que adquire e processa dados de quatro hidrofones. Na fase final, serão executados testes de campo e experiências num ambiente enclausurado, como o tanque do DEEC, seguido de um teste em ambiente real, em mar aberto.

Abstract

Robotic programmable devices such as Autonomous Underwater Vehicles (AUVs) are great means for underwater exploration, as they are capable of executing long term missions with many possible applications and goals. In this regard, the concept of mule AUVs arises as a valuable mechanism to periodically collect data from survey AUVs during the missions. In order to achieve this, a robust localization and positioning system needs to be implemented allowing the mule AUV to find the other vehicle and draw near it efficiently.

The present dissertation focuses on the implementation of a system which estimates the relative position between AUVs through the Ultra-Short Baseline (USBL) method. The technique relies on accurate estimation of the phase difference between signals received in a hydrophone array.

After implementation and validation of the mentioned system, it will be integrated in an existing mechanism which was specifically designed to acquire and process data from four hydrophones. In the final stage, field tests and experiments will be executed in a closed environment such as DEEC's tank, followed by a real environment test in open sea.

Contents

List of Figures

List of Tables

Abbreviations

AUV	Autonomous Underwater Vehicle
BPSK	Binary Phase Shift Keying
CC	Cross-Correlation
DEEC	Departamento de Engenharia Electrotécnica e de Computadores
FIM	Fisher Information Matrix
FPGA	Field-Programmable Gate Array
FSK	Frequency-Shift Keying
GCC	Generalized Cross-Correlation
HDL	Hardware Description Language
LBL	Long Baseline
LOS	Line-of-sight
MF	Medium Frequency
ML	Maximum Likelihood
RMS	Root Mean Square
RSSI	Received Signal Strength Indicator
SBL	Short Baseline
SNR	Signal-Noise Ratio
TDE	Time Delay Estimation
TDoA	Time Difference of Arrival
ToA	Time of Arrival
ToF	Time of Flight
USBL	Ultra-Short Baseline

Chapter 1

Introduction

1.1 Context and Motivation

Today, the deep blue ocean still represents a relevant topic of research in the scientific community as it constantly rises new unexplained mysteries. Up to now, only 15% of the entire ocean floor is mapped based on collected data [1]. As such, it seems essential to create efficient research tools to improve the discovery of information.

Robotic autonomous underwater vehicles (AUVs) are great means for diverse applications in underwater exploration using variable resource requirements and duration, such as monitoring structures installed in shallow waters or exploring the deep ocean floor for scientific purposes. Particularly in long-term missions, the AUV is usually deployed using a docking system and it navigates underwater until the end of the mission, when it returns to the base station. Thus far, the data that is being collected is typically not accessible by any processing system or researchers.

A method that is used to resolve this limitation is employing additional mule AUVs, whose goal is to travel near the survey AUV, collect its data during the mission's term and return in a relatively short time period. This allows the data to be periodically processed during the mission, which facilitates the definition of future courses for the mission, such as shortening its duration or sending additional commands. In the mentioned localization system, high accuracy is key, as it avoids high energy consumption, saves up time in the inherently slow global process and avoids missing the AUV's underwater localization.

The described process can only be achieved if the mule AUV is able to locate the other AUV and draw near it. For that reason, a USBL (Ultra Short Base-Line) system will be implemented using an array of four hydrophones as acoustic receiver. This makes it possible to explore the difference among times of arrival of an acoustic signal to many hydrophones, allowing the calculation of the angle of arrival of the acoustic signal and thus the direction that the mule AUV should navigate. Additionally, using a synchronized transmission from the AUV being located, the mule AUV can also determine the distance to the acoustic source located in the survey AUV and thus its relative position to the mule AUV.

This dissertation intends to continue the work developed previously [2], in which a platform was created to acquire and process data from four hydrophones. The system to be implemented is carefully explained in the present document.

This research work falls under the scope of activities developed by the Center of Robotics and Autonomous Systems of INESC TEC. It is integrated in the GROW project which focuses on exploring the use of AUVs as data mules for long duration missions.

1.2 Objectives

The work aims to implement a system capable of determining the angle of arrival of known encoded acoustic signal and study processes to correct errors resulting from the deformation of propagation direction of the acoustic waves. In order to achieve that, it is proposed the implementation and validation of a digital signal processing system for FPGA technology, which determines the difference between the times of arrival of an encoded acoustic signal to four hydrophones. Thereafter, a software script will be able to take the system's output in order to estimate the intended angle of arrival. The system is then analyzed and methods are studied in order to improve the estimation process. Finally, the implemented system is validated experimentally with field tests.

1.3 Document Structure

The present document is partitioned into x chapters, which are summarized in this section.

Chapter 2

State of the Art

This chapter presents the fundamental concepts of underwater acoustics engineering for localization and positioning of aquatic autonomous vehicles.

2.1 Underwater acoustic channel

Although satellite based navigation systems are the most commonly used for positioning and localization at the air, the used radio signals are highly absorbed by the water and thus inappropriate for underwater localization and also for communications. Therefore, the state of the art solutions for long range localization and communications rely on the propagation of acoustic signals.

The natural limitations of acoustic channels combined with the properties of an underwater environment, result in challenges and limitations in developing communication and localization systems [3]:

- Long propagation delays;
- Variable speed of the acoustic signals;
- Reference nodes may have different drifting rates from each other due to water currents, which leads to uncertainties on the definition of absolute times and synchronization;
- Limited bandwith
- Signals are bended due to sound speed variation along the water column and shadowed in many different surfaces, which may lead to the incorrect detection of the line-of-sight (LOS) signal;
- Attenuation and asymmetric signal-to-noise ratio, which arises from SNR depending on depth and frequency with complex behaviors that depend on the characteristics of the environment;

2.1.1 Speed of sound

The oceanic environment has a complex sound propagation model, as it comprises many variants in order to realistically represent underwater acoustics.

Acoustic signals' propagation speed is mainly related with two factors: compressibility and density. The water density can be characterized by the temperature, salinity and pressure,which is associated with depth. Figure 2.1 exhibits a generic sound speed profile in relation to depth. The water surface is commonly a mixed layer which results in an approximately constant sound speed. After this layer, it suffers a significative decrease, usually reaching the lower tangible speed, which results from the variation of temperature that characterizes the thermocline layer. From that point forward, pressure is the greatest influencer on the speed of sound, so it increases relatively proportionally to depth .

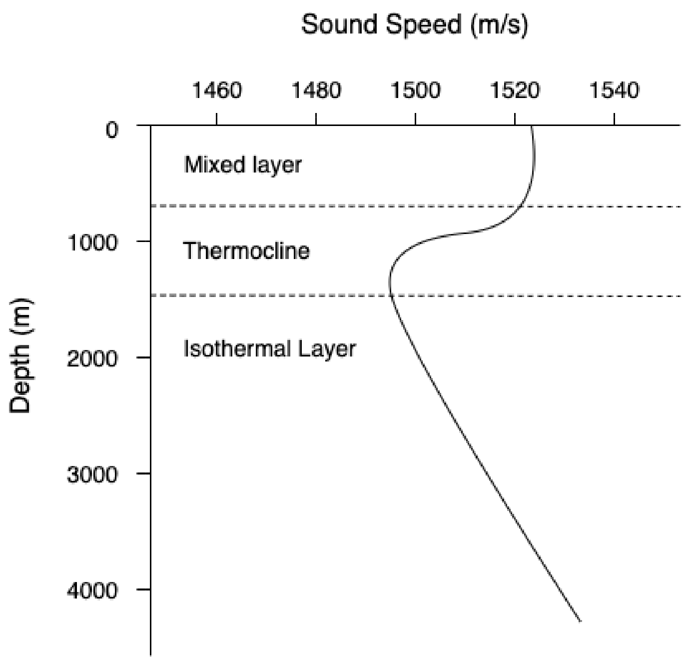

Figure 2.1: Generic sound speed profile

The empirical equation 2.1 [4] is a simplified translation of the behavior of the sound speed c in meters per second, with relation to the temperature T in ^{o}C, the salinity S in parts per thousand and the depth z in meters.

$$c = 1449.2 + 4.6T - 0.055T^2 + 0.00029T^3 + (1.34 - 0.01T)(S - 35) + 0.016z \tag{2.1}$$

2.1.2 Multipath

Multipath occurs when a transmitting signal suffers reflection or refraction in a surface (e.g. water surface, ocean floor, dock's wall), leading to a change in its original characteristics. This phenomenon can affect the propagation speed, the energy and the total distance that the signal was predicted to travel. These altered signals in conjunction with constant movement of the receiver makes it more complicated to accurately estimate the distance between the transmitter and the receiver, as well as determine the line-of-sight signal.

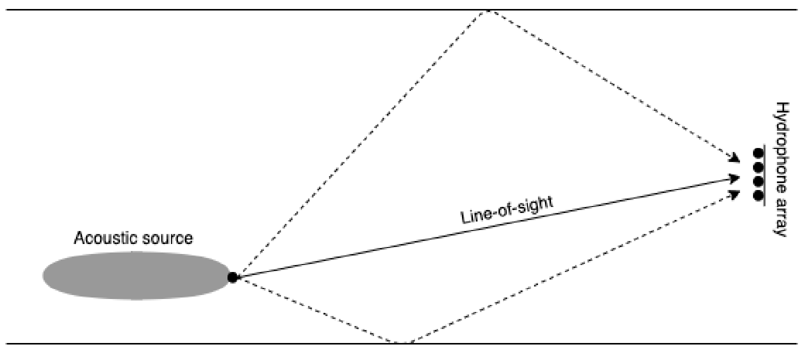

Figure 2.2: Multipath

In consequence, the underwater acoustic channel is qualified as a non-minimum phase system because it produces time-variant output responses.

2.1.3 Doppler Effect

In a communication and localization system between two entities moving with non-zero relative velocity, if a transmitter sends a signal with a certain operation frequency to the receiver, then the perceived frequency by the receiver will suffer a shift from the original signal. This frequency difference is expressed as a Doppler shift and explained by the Doppler Effect.

The magnitude of the generated frequency shift can be expressed as a ratio 2.2, where the transmitter-receiver velocity is compared to c, the speed of sound [5].

$$a = \frac{v}{c} \tag{2.2}$$

Autonomous Underwater Vehicles (AUVs) usually move with velocities in the order of few meters per second. Therefore, the a factor mentioned above has a significant value and needs to be considered when implementing synchronization systems, as well as developing estimation algorithms.

In certain localization and communication systems, it is critical to correct the Doppler effect because data can be compromised (e.g. FSK modulated signals, in which information is codified into frequency changes). A simple Doppler compensation process was proposed in [6], in a system to detect phase-modulted binary sequences using cross-correlation.

This phenomenon can also be explored to determine the relative velocity between two devices, by measuring the frequency deviation with respect to the frequency expected to be received.

2.1.4 Attenuation and signal-to-noise ratio

When considering underwater communication systems, it is essential to quantify the attenuation of the channel, i.e. the part of the signal's energy which is absorbed by the involving surrounding. In underwater channels, this absorbance is frequency variable and it is also dependent on physical characteristics of the water, as salinity and temperature.

The underwater acoustic channel has a particular model that describes its attenuation path loss $A(d,f)$, given in logarithmic scale by equation 2.3 [7].

$$10\ log(A(d,f)) = 10\ k\ log(d) + d\ 10\ log(a(f)) \tag{2.3}$$

From the equation, d is the distance from the transmitter to the receiver in kilometers (Km), f is the operating frequency in kilohertz (KHz), $10klog(d)$ represents the spreading loss which describes how the sound level (in decibel, dB) decreases as the sound wave spreads, $d10log(a(f))$ is the absorption loss that a signal suffers during its propagation path, k is the spreading factor which is related with the considered configuration (e.g. cylindrical, spheric, etc.), $a(f)$ is the absorption coefficient that can be obtained through the equation in [7].

Noise is another factor that is considered when analyzing a real underwater acoustic channel, as it defines the signal-to-noise ratio (SNR) that characterizes the channel. The SNR is dependent on the attenuation level which increases with frequency, and the noise which decays with frequency. Consequently, the SNR varies over the signal bandwidth and it is asymmetric. The equation 2.4 [5] expresses this relationship, where $S_d(f)$ represents the power spectral density of the transmitted signal.

$$SNR(d,f) = \frac{S_d(f)}{(A(d,f))\ N(f)} \tag{2.4}$$

2.2 Range estimation for underwater localization

Underwater localization takes into consideration the distance between the target object to track and the reference point. As consequence, it is always relevant to apply methods which easily and effectively determine this range.

There are two main types of techniques that are used to achieve such objective: the Received Signal Strength Indicator (RSSI) and the Time Delay Estimation (TDE).

2.2.1 Received Signal Strength Indicator

The Received Signal Strength Indicator (RSSI) method is based on the strength of the signal that reaches the target. It determines the distance between the target and the reference node by analyzing the received signal strength and comparing it with an underwater attenuation model which is range dependent [4].

Since the underwater acoustic channel suffers from multipath, time variance and high overall path loss, the RSSI technique is not adequate for underwater applications.

2.2.2 Time Delay Estimation

Time Delay Estimation (TDE) mechanisms use a pair of nodes, the target and the reference point, to measure the range between them. This distance is based on the time that it takes for a signal to travel from the reference point to the target.

There are three main categories that devide TDE methods, which are Time Difference of Arrival (TDoA), Time of Arrival (ToA) and Time of Flight (ToF).

2.2.2.1 Time of Arrival

Time of Arrival (ToA) is interpreted as the time delay between the transmission of a signal in the reference node until its reception on the target node. Although this is the conceptually simplest method to employ, it requires synchronization between the nodes since the target entity needs to know the instance when the signal was sent to be able to calculate the difference.

Considering a generic transmitted signal *s(t)*, the received signal can be expressed as 2.5, where τ represents the time of arrival and *n(t)* is white noise with zero mean [8].

$$r(t) = s(t-\tau) + n(t) \tag{2.5}$$

2.2.2.2 Time of Flight

Time of Flight (ToF) measures essentially the round-trip time communication between two nodes. The target node sends a signal to the reference node, which has an integrated transponder that responds transmitting a signal back to the target. The ToF is then estimated as the time interval from the moment the first signal is transmitted until the moment the second signal is received by the same node.

This method may be used without additional synchronization systems as it assumes that the response signal is sent immediately after the received one and the intrinsic transmitting delays are known.

The accuracy of this technique depends mainly on the environment conditions, which include the water properties and the surrounding reflection surfaces which cause multipath. Therefore, the mechanism is susceptible of variable errors according to the location and characteristics of its employment.

2.2.2.3 Time Difference of Arrival

The Time Difference of Arrival (TDoA) is a technique that compares the time of arrival of a signal to different hydrophones in order to estimate the angle of arrival of the acoustic signal. The array of reception hydrophones have known determined positions among them so that is is possible to compare the different times of arrival or phase differences. This method can be employed using a uni-directional signal or a round trip communication.

There are several algorithms and mathematical models that can be employed to execute the TDoA method, such as Cross-Correlation and Maximum Likelihood.

- **Generalized Cross-Correlation**

  The Generalized Cross-Correlation (GCC) method is used to generically represent the relationship strength between two signals.

  Considering two distanced hydrophones in the same environment and an acoustic source *s(t)*, *x1(t)* and *x2(t)* are the signals received by each of the two hydrophones. The equations 2.6 and 2.7 [9] express the mentioned signals in relation to *w1(t)* and *w2(t)* which are Gaussian noise coefficients uncorrelated with the source, τ that represent the delay and α which is an attenuation function.

$$x1(t) = s(t) + w1(t) \tag{2.6}$$

$$x2(t) = \alpha s(t-\tau) + w2(t) \tag{2.7}$$

$$\tag{2.8}$$

  From these expressions, the generalized cross-correlation function between signals *x1(t)* and *x2(t)* is given by 2.9. The $G_{x1x2}(f)$ is the spectrum of the cross-correlation. The $\psi(f)$ represents a prefilter and it is essentially the distinctive parameter that originate various different methods of cross-correlation, since it should depend on different environments and properties as SNR.

$$R_{x1x2}(\tau) = \int_{-\infty}^{\infty} \psi(f) G_{x1x2}(f)\, e^{i2\pi f\tau} df \tag{2.9}$$

$$T = \tau_{max}[R_{x1x2}(\tau)] \tag{2.10}$$

  Finally, the maximum value of $R_{x1x2}(\tau)$, expressed in 2.10, is the so called correlation peak and provides information about the time delay τ which is the main matter of Time Delay Estimation.

- **Cross-Correlation**

  After approaching the generalized method of cross-correlation, it is possible to better understand the Cross-Correlation (CC) method. There are two main variations of CC [9], which are the slow cross-correlation in the time domain and the fast cross-correlation in the frequency domain. The second approach is based on the Fast Fourier Transform as it locates the peak by analyzing frequency similarities between the signals.

  Th Cross-Correlation technique uses a prefilter $\psi(f)$ equal to 1, as it is the simplest method of its kind.

- **Maximum Likelihood**

The Maximum Likelihood (ML) method is a variation of Cross-Correlation which uses the prefilter $\psi(f)$ represented mathematically by 2.11, where $\gamma_{12}(f)$ is a function of spectrum of cross-correlation $G_{x1x2}(f)$ and spectrum of auto-correlations $G_{x1x1}(f)$, $G_{x2x2}(f)$ as expressed in 2.12 [9].

$$\psi(f) = \frac{|\gamma_{12}(f)|^2}{|G_{x1x2}(f)|[1-|\gamma_{12}(f)|^2]} \tag{2.11}$$

$$|\gamma_{12}(f)|^2 = \frac{|G_{x1x2}(f)|^2}{G_{x1x11}(f).G_{x1x11}(f)]} \tag{2.12}$$

There is also a version of ML that uses the power spectral densities of the signals, which can be helpful for calculations in various applications.

2.3 Localization estimation

In networks with multiple nodes is typical to use localization estimation to establish position relationships between elements. The operation principal is usually to have a set of reference nodes with known positions so that it is possible to determine the relative positions between each reference node and the target.

An extensive comparison of different localization schemes for underwater sensors networks can be consulted in [10].

2.3.1 Triangulation

Triangulation is a method of localization based on the measurement of angles which are related to the reference beacons and the target object.

2.3.1.1 Three-Object Triangulation

The simplest method of this category is the Three-Object Triangulation, which considers a configuration as illustrated in figure 2.3. It is assumed that the location of the beacons is pre-configured and the environment is obstacle-free. λ_{12} is the angle formed by the intersection of the straight lines [O,1] and [O,2]. Similarly, λ_{31} is the angle formed by the intersection of the straight lines [O,1] and [O,3]. Using these two sets of nodes, we can trace circumferences that include their coordinates and as a consequence their intersection will correspond to the location of the target.

Although this is a very straightforward technique to implement, it does not cover all possible scenarios, namely when the three beacons and the object are all placed in the same circumference or when the environment has obstacles between nodes.

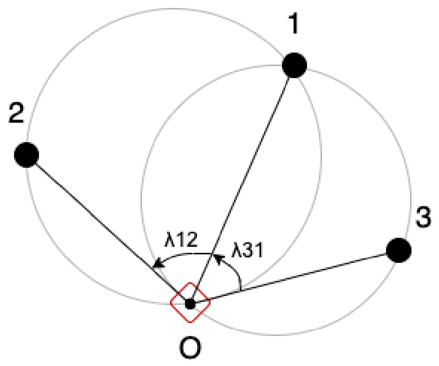

Figure 2.3: Three-Object Triangulation

2.3.1.2 Geometric Triangulation algorithm

A more complex method relies on the Geometric Triangulation algorithm.

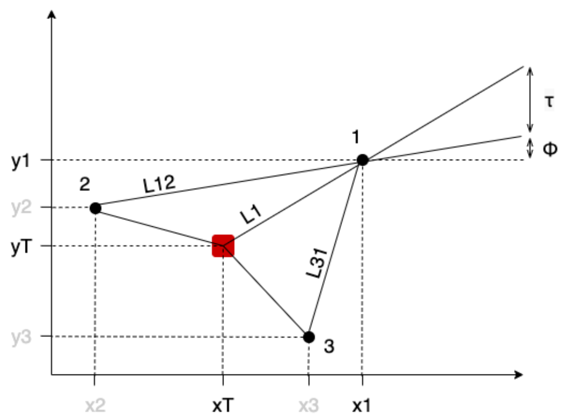

Figure 2.4: Geometric Triangulation algorithm

Considering a Cartesian plane with defined lengths L1, L12 and L31, as shown in image 2.4, it is possible to establish trigonometrical relationships that estimate the location of the object within the created triangular areas. The position of the target is given by coordinates (xT,yT) and can be calculated through equations 2.13 and 2.14. (x1,y1) represents the location of beacon 1 and L1 is the distance between this beacon and the object. The trigonometric relationships for calculating the mentioned variables can be consulted in [11].

$$xT = x1 - L1 * cos(\phi + \tau) \tag{2.13}$$

$$yT = y1 - L1 * sin(\phi + \tau) \tag{2.14}$$

2.3.2 Trilateration

Trilateration is a technique that does not rely on calculations using angles but instead it uses distances to locate an object.

Considering a scenario with three reference beacons, the distance between the target and each one of the beacons is taken as the radius of a circumference. By doing this, it is possible to obtain three circumferences that intersect each other. With only two circumferences, there are two possible locations for the object, however, when added the third circumference the exact location is obtained. The 2D coordinates are obtained by solving systems of equations with the circle equation 2.15 [12], where (x_i, y_i) is the beacon coordinates and r_i is the distance between the beacon and the object.

$$(x - x_i)^2 + (y - y_i)^2 = r_i^2 \tag{2.15}$$

Trilateration is commonly used in underwater acoustic localization, as it used to find a relative position of the target in two dimensions and additionally determines the depth as third dimension, by using a pressure sensor with high accuracy.

2.3.3 Multilateration

Multilateration is a generalization of the trilateration technique, as it uses the same conceptual principal with multiple reference beacons instead of exactly three. In this method, the employment of *n+1* nodes will allow to determine *n* coordinates [13]. For example, determining the position (x,y,z) of a target, would require to resolve a system of equations using 2.16. (x_i, y_i, z_i) is the coordinates of the beacon and d_i is the distance between the beacon and the target.

$$(x - x_i)^2 + (y - y_i)^2 + (z - z_i)^2 = d_i^2 \tag{2.16}$$

Distributed mechanisms, such as multilateration, are usually divided in three phases of positioning [10]:

- Distance estimation between the reference nodes and target object, usually using TDoA or ToF mechanisms;
- Position estimation, usually obtained by solving a system of linear equations through mathematical efficient techniques;
- Final refinement of the measurement in order to improve accuracy.

As an alternative to solve localization issues using circumferences, multilateration can also take advantage of a hyperbola-based localization method. Considering a target at (x,y) and three reference beacon with coordinates (x_i, y_i), (x_j, y_j) and (x_k, y_k), we have that the difference between times of arrival t_i and t_j to nodes i and j, respectively, can be related to the distance between nodes, as expressed in 2.17 [13]. d_i and d_j are the distance from node i and j, respectively, to the target object.

$$d_i - d_j = c * (t_i - t_j) = \sqrt{(x - xi)^2 + y - yi)^2} - \sqrt{(x - xk)^2 + y - yk)^2} \tag{2.17}$$

2.4 Positioning Systems

Positioning systems are used to track the underwater position of a vehicle or other object, in relation to reference structures of transponders called *baseline stations*. These systems are classified based on the distance between the baseline stations. The configurations that will be explained are Long Baseline (LBL), Short Baseline (SBL), Ultra-Short Baseline (USBL) and the inverted versions of all above.

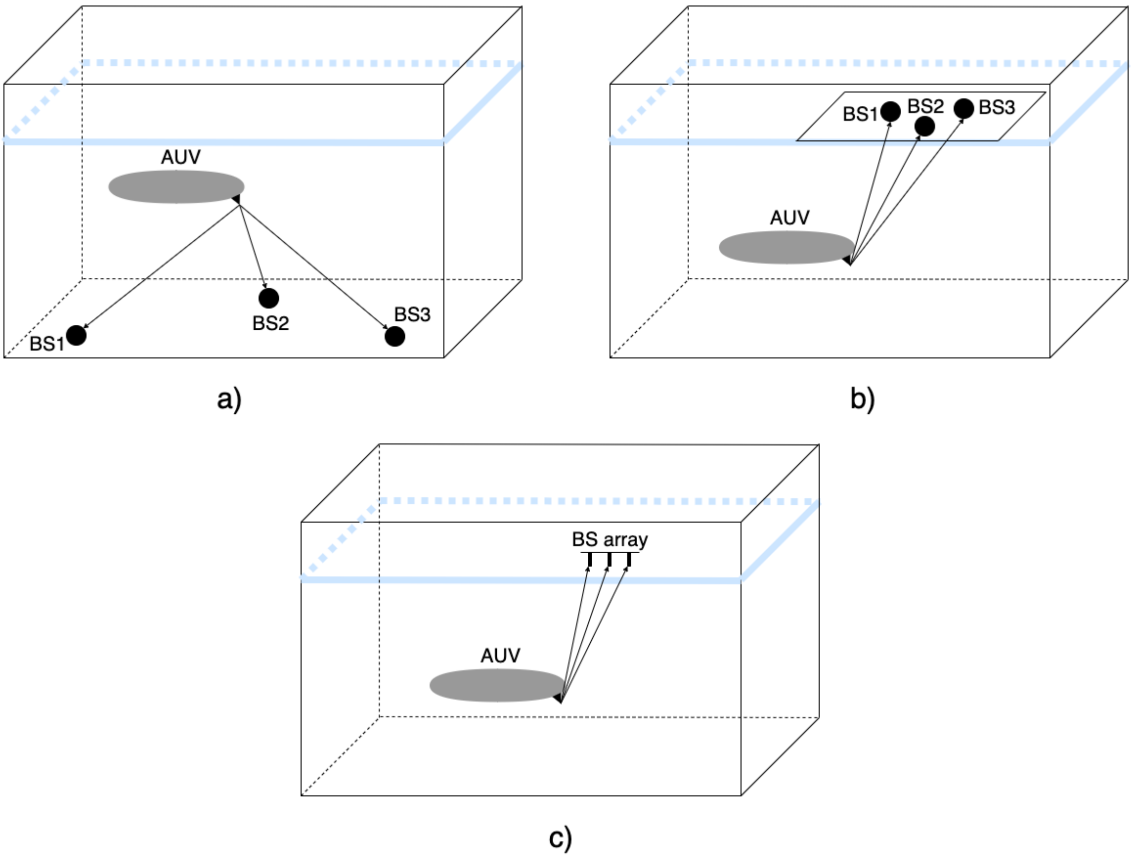

Figure 2.5: Generic configuration of: a) LBL; b) SBL; c) USBL

2.4.1 Long Baseline (LBL)

Long Baseline systems use a positioning method with large distances between baseline stations, with range typically from 50m to more than 2000m and usually similar to the distance between object and transponders [9]. A typical LBL configuration is represented in figure a) 2.5.

The LBL method uses at least three transponder stations deployed usually on the sea floor, allowing to execute trilateration. Additionally, a transducer is integrated on the object to be tracked.

A complete localization procedure starts with the vehicle sending an acoustic signal which is received by the transponders. Thereafter the transponders transmit a response and, by analyzing the Time of Flight of the communication, the system can determine the distance between the vehicle and each base station. Then the relative position of the vehicle is determined through trilateration. Additionally, if the transponders have known geographic positions, it is possible to infer the vehicle geographic position.

As this technique presents large distances between the object and the base stations, the typical 1m to few centimeters accuracy is considered to be high because it will not compromise the localization of the vehicle.

2.4.2 Short Baseline (SBL)

Short Baseline systems are characterized by having distances around 20m to 50m between baseline stations [3] and use an operation procedure similar to the LBL method. However, the transponders are usually placed in a moving platform, which assures a fixed relative position between them. A typical SBL configuration is represented in figure b) 2.5.

The position of the vehicle to be tracked can be determined by translating the Time of Flight between the multiple transponders and the object into a distance value, which is achieved by equation 2.18 [14]. The t_i corresponds to the propagation time of the signal from the vehicle to the ith transponder, c is the speed of sound, [x_{b_i}, y_{b_i} and z_{b_i}] is the coordinate position of the transponder.

$$\sqrt{(x_{b_i}-x)^2+(y_{b_i}-y)^2+(z_{b_i}-z)^2} = c \, * \, t_i \tag{2.18}$$

In a SBL system, when the distance between baseline stations is increased the accuracy improves and, contrarily, when the mentioned distance decreases the accuracy deteriorates, which can raise some deployment challenges.

2.4.3 Ultra-Short Baseline (USBL)

Ultra-short baseline systems are composed essentially by one baseline station, with an array consisting of several traducers distanced typically less than the wavelength [15], and a transponder integrated on the object to be tracked. It is usually used in underwater positioning in shallow areas of the sea, as represented in figure c) 2.5.

Similarly to the previously mentioned procedures, the USBL positioning method relies on the Time of Flight of the exchanged signals. However, the traducers are too spatially close from each other to execute an accurate trilateration. Instead, it is measured the phase difference or time-delay difference of the received signal between every traducer, in order to estimate the azimuth and distance to the acoustic source.

Assuming a three dimensional scenario for the positioning system, as represented in figure 2.6, the object's coordinates are given by equations 2.20, 2.21 and 2.22 [16]. The λ corresponds to the wavelength of the of the transmitted signal which depends on its operation frequency, f, and it is affected by the speed of sound c, as represented equation 2.19. The d represents the distance between hydrophones, ψ_{12} and ψ_{22} are the phase difference between H2 and the other two hydrophones, H is the height of the target object, X is the distance of the target along the x-axis direction, Y is the distance of the target along the y-axis direction and l is the slant distance of the target to the hydrophone.

$$c = f * \lambda \tag{2.19}$$

$$l^2 = X^2 + Y^2 + H^2 \tag{2.20}$$

$$\psi_{12} = \frac{2\pi}{\lambda}[\sqrt{l^2} - \sqrt{(d-X)^2 + d^2 + H^2}] \tag{2.21}$$

$$\psi_{22} = \frac{2\pi}{\lambda}[\sqrt{l^2} - \sqrt{X^2 + (d-Y)^2 + H^2}] \tag{2.22}$$

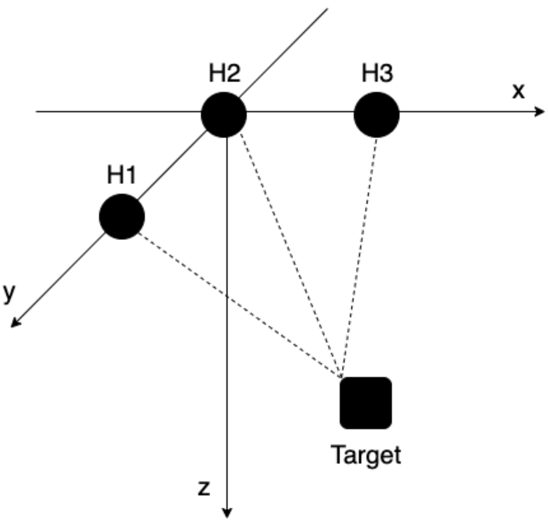

Figure 2.6: USBL system configuration

This is a broadly used technique due to its convenient set up, which allows to have predefined measurements in the order of tens of centimeters and does not require AUV navigation area for the deployment. However it presents the lowest accuracy, comparatively with LBL and SBL, since an error of few centimeters can be realistically corresponding to an inaccuracy of several meters in the position of the object to be tracked.

2.4.4 Inverted Systems

All the previously mentioned positioning techniques use a configuration in which the vehicle to be tracked has a single transducer and there is an external set of transponder to determine the positioning of the said object. However, there is the possibility to benefit from the inverse configuration in some applications. Therefore, there are also the iLBL, iSBL and iUSBL methods, which have the same operation principals as LBL, SBL and USBL, respectively.

2.5 Commercial Solutions

There are several commercial solutions for underwater positioning using the ultra-short baseline method. In this section, it will be presented some of the available devices in the market, indicating their main properties and capabilities. Table 2.1 summarizes the systems with most relevance to the present work. The Medium Frequency (MF) bandwidth is attributed to devices whose manufacturer did not specified the actual frequency range.

Evologics produces the S2C R USBL series of acoustic modems [17], with Sweep Spread Carrier (S2C) technology [18] which uses a broad frequency range to propagate over large distances with reduced noise. The devices have a fixed 0.01m slant range accuracy and a 0.1 degree bearing resolution. These are essentially divided into two groups:

- High speed mid-range devices: contains the 18/34 transceivers family [19], which presents various options for the USBL antenna beam pattern and it is optimal for transmission in horizontal channels.

- Depth rated long-range devices: includes the 12/24 transceiver [20], which have a directional (70 degrees) USBL antenna and it is optimal for transmission in vertical channels.

Sonardyne markets the Ranger 2 systems. The Micro-Ranger 2 [21] is very easy to use without previous experience and it is appropriate for shallow waters, achieving accuracy of 0.2%. The Mini-Ranger 2 is ideal for nearshore missions and it is used for simultaneous tracking of various mobile targets, whose position is updated every 3 seconds.

Applied Acoustics offers the Easytrak USBL Systems, which includes the processing software for estimating the position. The Alpha Portable 2655 consists in a very compact structure that includes an array transducer and is capable of reaching a 10cm slant range resolution and a 2 degree RMS.

Kongsberg produces the HiPAP family of transducers [22], which can use the Cymbal acoustic protocol (PSK) or the frequency shift (FSK) modulation technique. Particularly the HiPAP 352 is the model with higher number of active transducers and is able to reaches 0.02m of range accuracy.

Company	System	Bandwidth(kHz)	Connection(kbps)	Range(m)
Evologics	S2C R 18/34D USBL	18-34	up to 13.9	3500
	S2C R 12/24 USBL	12-24	up to 9.2	6000
Sonardyne	Micro-Ranger 2	MF	0.2-9	995
	Mini-Ranger 2	MF	0.2-9	995
Applied Acoustics	Easytrak Alpha Portable 2655	MF	n.d.	500
Kongsberg	HiPAP 352	21-31	n.d.	5000

Table 2.1: Overview of commercial solutions

2.6 Angle of arrival determination

methods for calculating signal's angle of arrival

2.7 Optimization of sensor configurations

When evaluating the performance of a localization system which integrates a multiple sensor configuration, it is essential to resort to widely used methodologies to prove its validity and accuracy. This section is dedicated to explore some commonly employed methodologies.

2.7.1 Crámer-Rao lower bound

In this thesis, it is conducted a study based on the Crámer-Rao lower bound, which is generally used to generate a *so-called uncertainty ellipse* [23] that represents the spatial variance distribution of the estimated position. The overall desired result is to find the minimum variance value that is related to the chosen configuration geometry, which indicates that it is the optimal solution for estimating a certain position. This method utilizes the Fisher Information matrix (FIM), which measures the quantity of information that can be extracted from an observation vector about a certain parameter.

In order to avoid loss of generality, it is considered a set of N sensors and a settled position for the target, the acoustic source, defined by $s_t = [x_{s_t}, y_{s_t}, z_{s_t}]^T$. In addition, the position of each sensor is defined as $r_i = [x_{r_i}, y_{r_i}, z_{r_i}]$ and, consequently, the measurement of distance between each sensor and the source is defined as $\mathrm{d}_i = ||s_t - r_i||$.

Thereafter, the observations vector will be formulated containing the observed times-of-arrival (ToA) of the signal from the acoustic source to each one of the hydrophones, considering their geometric position. These times contain a noise vector component, which can be approximated to to a Gaussian distribution $n_i \sim \mathcal{N}(\mu, \sigma^2)$. The samples can be calculated through the expression 2.23, where it is considered an initial time of arrival t_0. Additionally, c represents the sound speed underwater.

$$t_i = t_0 + \frac{||d_i||}{c} + n_i \tag{2.23}$$

After having the observations matrix, it is established the condition to formulate the Fisher Information matrix, $I(d)$, which results into equation 2.24.

$$I(d) = \nabla_d t(d)^T \, \Sigma^{-1} \, \nabla_d t(d) \tag{2.24}$$

$\nabla_d t(d)$ is the gradient matrix of the observations vector regarding d_i, whereas Σ is the covariance matrix, in which the diagonal contains the standard deviation of the components of each noise vector, construed as $(\sigma_1^2, \sigma_2^2, ..., \sigma_N^2)$.

Thereby, all conditions are established to proceed to the actual calculation of the Fisher Information matrix. After formulated, it will indicate the quantity of information that a certain sensor configuration can give about a position in space. Hence the goal is to obtain the maximum achievable information. By calculating the determinant of FIM it is possible to deduce the minimum *uncertainty ellipsoid* and therefore the configuration's best possible performance. Therefore, the optimal solution is given by the maximum output of the determinant of FIM.

Additionally, it is possible to detail this information by calculating the actual size of the axis that compose the *uncertainty ellipsoid*. This is achieved by calculating the square mean root of the eigenvalues of $I(d)$, which correspond to each axis size.

Further explanation about the methods used in a deeper exploration of the Crámer-Rao lower bound can be consulted in [23], which serves as guide to investigate other scenarios of application of this theorem. However, the mentioned concepts were all the necessary for the approach on this dissertation .

This same process is adopted in this dissertation. All steps specifically taken for this study are declared in section 5.1 of the present document.

2.7.2 Optimal design and optimality criteria

When contemplating system designs, the optimal solution for a problem is generally a subjective matter which depends on the chosen principal. Following this idea, we can define optimal designs as experimentally generated designs of various types of systems which are usually optimal for a targeted statistical model and are modelled by a specific optimality criterion. These criteria can be organized in four distinct groups [24]:

- **Information-based** : comprehends all criteria that are related to the Fisher information matrix $X'X$. Some of the criteria which fits into this category are A, D, E and G-optimality.

- **Distance-based** : includes criteria which depends on the distance $d(x,A)$ from a point x in the Euclidean space $\mathbb{R}^p$ to a set $A \subset \mathbb{R}^p$. U and S-optimality are integrated in this category.

- **Compound design** : combine different adjusted criteria in different weighted proportions in order to meet a desired statistical function.
- Other : all criteria which do not fit in the previous three sets can be encompassed in a fourth general set.

The most relevant category for the present work is the information-based criteria, since we want to maximize the information that can be extracted from a certain design and we do not need to minimize the distances between the receptors and the source. Therefore some of the most commonly used criteria will be better explained in the following subsections.

2.7.2.1 D-optimality

2.7.2.2 E-optimality

2.7.2.3 A-optimality

2.7.2.4 G-optimality

Chapter 3

Research Problem

This chapter intends to clarify the problem addressed by the present dissertation.

3.1 Problem Statement

As previously mentioned in chapter 1, it is considered a scenario where an AUV is taking part on a long-term underwater mission. When it is in course, the moving survey AUV periodically sends known signals to the surface with a pinger, so it can be identified. The mule AUV, which is provided with a three dimensional array of hydrophones, receives the signal and estimates the position of the other AUV to navigate near it. The described communication system is illustrated in figure 3.1.

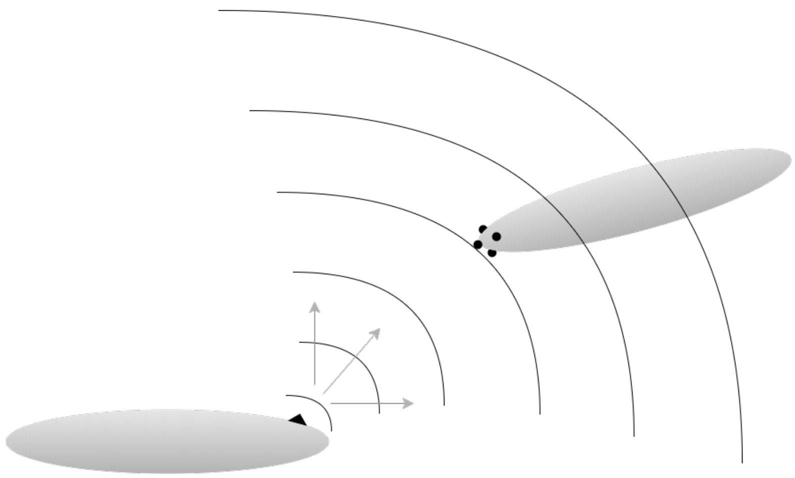

Figure 3.1: Communication System

This partial system was developed in previous dissertations and research work, which can be better understood in [2]. Briefly, the system consists on a transducer of four hydrophones forming a 3D array deployed on the mule AUV. This array will receive the same signal wave front. The system then calculates the cross-correlation between the received and expected signals, which is a BPSK modulated binary sequence. The cross-correlation peak indicates the distance between AUVs and it is calculated with timing resolution corresponding to 1 sampling period of the acquired signal, which in the developed systems corresponds approximately to 6mm (with a sampling frequency of 244kHz).

Since we are referring to an USBL system and due to the limitations in dimension of the AUV that will integrate this system, the hydrophones have to be placed within a few centimeters from each other. For this reason, the obtained time resolution by using only the cross-correlation, corresponding to a maximum distance accuracy of approximately 6mm, will not be enough for the calculation of the angle of arrival of the sound wave. Thus, in this thesis it is intended to refine this measurement by additionally calculating the phase differences of the arriving signals to each hydrophone.

Upon having this measurement refined, the information of the phase difference between hydrophones, as well as additional data from modules already implemented, will serve as base to develop a software mechanism that estimates the angle of arrival of the received signal to the hydrophone array.

Finally, as an effort to improve the underwater localization system, a set of tests have to be performed in order to evaluate the robustness and estimation accuracy of the developed system. This study intends to prove the hypothesis declared in 3.2 and consequently respond to some of the defined research questions.

3.2 Hypothesis and Research Questions

This dissertation intends to complement previous research work by adding the design of an integral hardware model and respond to a core research hypothesis which serves as fundamental investigation purpose.

The first part of the developed work focuses on the practical implementation of a HDL model which has as premise the following idea: *"Implementing a system that utilizes the phase differences between the arriving signals to an array of hydrophones, increases the accuracy of the time of arrival determination of the current system, which consequently improves the angle of arrival estimation."*

The second part of the research work focuses on the study and experimentation with methods that improve the localization accuracy for underwater applications. This research hypothesis can be stated as:

"Using a real-time dynamic reconfigurable hydrophone array improves the underwater localization accuracy"

Attending the proposed hypothesis, the topics that are intended to be explored and discussed in this thesis's work can be summarized in the following research questions:

- **RQ1:** *How should a system be implemented so it is capable of calculating phase differences between arriving signals at four different hydrophones and, simultaneously, be compatible with the available space in the FPGA?*
- **RQ2:** *What method should be adopted in order to efficiently estimate the angle of arrival of a signal to an array of four hydrophones?*
- **RQ3:** *What metrics should be used to evaluate which hydrophone configuration is optimal for a certain angle of arrival?*
- **RQ4:** *How should the system be developed in order to improve the vision angle of the hydrophone array?*

These questions summarize the main topic points which are explored in the scope of this thesis and are the essential inquiries that it intends to answer.

3.3 Validation Methods

The validation of scientific work is a key factor to demonstrate how reliable and effective it is. In this thesis, three essential methods are used to validate the functionality of the developed techniques:

- **Simulation**

  The considered immediate approach to evaluate the functionality and behavior of the system consists in creating a set of simulation procedures which are as close as possible to the real environment and the physical system. These simulations were made as MATLAB scripts carefully designed to integrate realistic parameters, such as expected environment noise and other limitations.

- **Scientifically recognized methods**

  When composing a system, it can be useful comparing the studied approach with widely used methods which are recognized in the scientific community as robust and trustworthy. By doing this, we can gain a level of confidence in the developed system and in the obtained results.

- **Field experiments**

  After having the analytical methods and simulations coherent, it is essential then to test the system in a real environment in order to understand if the system still works correctly when real conditions are added. By testing it in a real application it is possible to take conclusions about its robustness and consider improvements or refinements for the system.

Chapter 4

Ultra-Short Baseline System

This chapter is dedicated to the presentation and overall explanation of the developed system, highlighting its capabilities, the used methodologies and overall design strategies. The system will be presented in two distinct sections. The first component is the HDL module, which falls into the spectrum of hardware design and requires insight on hardware development and good practices. The second section relies on software development to complement the functionality of the mentioned module, so that is possible to deliver the desired result.

4.1 HDL Module Architecture

The system which is proposed to be implemented in this research work has as input 4 signals which are received by each hydrophone of the array, and outputs an average phase difference between all combinations of pairs of hydrophones.

- regras basicas de hardware development
- sistema sincrono, available clock cycles globais
- hardware limitations
- tamanho das entradas arg

1. Hilbert Filter
2. Cordic
3. phasediff
4. phasemean

4.1.1 Module components

apresentar esquema global menos pormenorizado

4.1.1.1 Hilbert Filter

$$H(f)(t) = \frac{1}{\pi}\int_{-\infty}^{\infty}\frac{f(\tau)}{t-\tau}d\tau \tag{4.1}$$

$$Imag_0 = x_{-1} * c_1 + x_{-3} * c_3 + x_{-5} * c_5 + x_{-7} * c_7 \tag{4.2}$$

$$Real_0 = x_{-4} \tag{4.3}$$

- matematica brevemente, equação base, resposta impulsional, ganho, coeficientes e ordem usada
- schematics
- explicar design decisions
- descrever brevemente flow do sinal no hardware

4.1.1.2 Cordic

- descriçao do que faz
- entradas e saídas, clocks, ROM

4.1.1.3 phasediff

-pequeno esquema
- 1 sub

4.1.1.4 phasemean

- pequeno esquema
- N accumulated

4.1.2 Analysis

present used resources
overall achievement

4.2 Position Estimator

The proposed position estimator uses vector algebra, the phase differences obtained from the system described in 4.1, synchronization elements and additional mechanisms that will be further explained in the present section.

4.2.1 Preliminary considerations

4.2.1.1 Number of sensors

For the estimation of the position in 3D space, a multilateration approach was used. As explained in 2.3.3, the concept of multilateration combines the information of the relative distances between multiple sensors and a target in order to locate it.

In the present case, a total of four sensors are needed so that it is possible to define the position of target. Using only two sensors, two possibility spheres are formed around these sensors whose intersection originates a circle that contains the location possible solutions. By adding a third sensor, this circle is intersected by another sphere which originates only two location possibilities. Finally, a fourth sensor is added so that it is possible to exactly differentiate which one of the two final solutions is the accurate location solution.

4.2.1.2 Phase Ambiguity

When the information about the time of arrival of a signal is available, it is relatively easy to estimate the range of the communication since there can be a direct conversion between them. However, when dealing with phase differences, there is no exact time notion, so it is necessary to start by defining a reference point.

Considering sinusoidal signals, when we have an array with four hydrophones spatially placed to form a 3D layout, the signal that is arriving to each hydrophone in different times consequently have different phases. However, since sinusoidal signals are periodic, this means that for different signal periods the same phase value is observed, i.e. the phase is ambiguous. It is possible to observe this phenomenon in figure 4.1. In this illustration, α represents the observable phase difference of hydrophone H_4 to the reference point H_1. However, the actual phase difference which is intended to obtain, Δp_4, is one period of the signal, λ, added to the observable phase α.

For this reason, it is crucial to consider that the phase difference is given by the obtained phase value added by the number of periods ahead from the considered reference period.

In the system under study, the sent signals work with a operation frequency of 24.4 kHz. The corresponding signal period is $T = \frac{1}{24400}$ seconds which, considering the underwater acoustic speed c equal to a standard 1500 m/s, the wavelength is approximately equal to $\lambda = \frac{T}{c} = 6.1cm$. Having this into consideration, after obtaining the time of arrival to each hydrophone given by the cross correlation instances, besides the reference one, it is possible to conclude if the phase shift is superior to one period by analyzing if the time difference is greater than the duration of one period

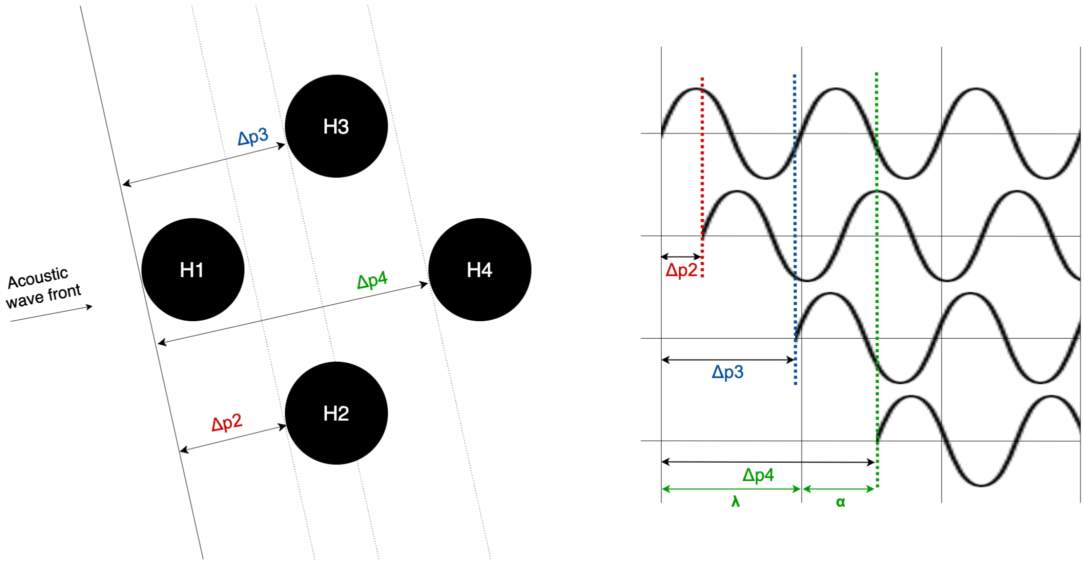

Figure 4.1: Phase difference to reference point and phase ambiguity

T. In figure 4.1, each mentioned time difference between H_1 and H_2, H_3 and H_4 is converted to the corresponding phase differences Δp_2, Δp_3 and Δp_4.

One possibility to solve phase ambiguity in this system would be to place the four hydrophones with a baseline spacing inferior to $\frac{1}{2}$ of a wavelength, since the maximum reached by phase difference is 180 degrees. This way it would be possible to immediately deduce the phase difference since it would always be contained in one period. However, positioning the hydrophones closer together leads to smaller values,causing a consequent increase on the estimation error due to varying environment conditions (briefly enumerated in 2.1). Additionally, since the hydrophones to be used in this system have a corresponding diameter of roughly half of a wavelength, they would not allow to execute the mentioned configuration and so this possibility will not be contemplated.

In order to compensate this phase ambiguity, a simple relation was developed which allows to calculate the absolute time difference between the moment a signal is received by hydrophone A, T_A, and when the same signal is received by a further hydrophone B, T_B. Figure 4.2 illustrates this association, where the represented sinusoidal waves correspond to the same signal arriving at hydrophones A and B. This correspondence uses the time stamps obtained by the correlation peaks combined with the calculated phase difference, that is determined in parallel, so that the measurement is more accurate. Equation 4.4 translates this relation, where t_1 and t_2 are the correlation peaks obtained from the signal arriving at hydrophone A and B, respectively, and so by rounding for the next integer number the difference between the correlation peaks, $t_2 - t_1$, we will obtain in which period, T, of signal in A will the signal in B arrive. Then the measurement is improved by subtracting a phase difference, $\theta_B - \theta_A$, so that the instant in which the signal is detected in hydrophone B can be defined.

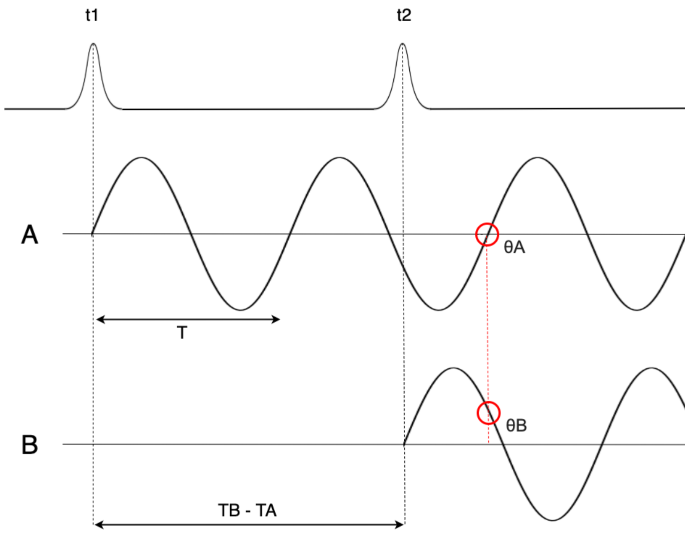

Figure 4.2: Ambiguity correction through correlation and phase difference

$$T_B - T_A = round(\frac{t_2 - t_1}{T}) - (\theta_B - \theta_A) \quad (4.4)$$

4.2.1.3 Position in relation to ToA

To better understand the location estimation of an acoustic source in relation to the position of a pair of hydrophones, we can initially adopt the two dimensional scenario of figure 4.3.

Considering two hydrophones at known relative positions $(-f,0)$ and $(f,0)$, we can model all possible acoustic source locations for a specific ToA through hyperbolas. This is due to the fact that, by definition, the sum of the distances from the focus of each hyperbole, where each hydrophone is placed, to any point of the hyperbolic geometry corresponds to a constant value. This means that, in figure 4.3, any point (x,y) that is contained in the hyperbole corresponds to a constant $|d_2 - d_1|$ value which, after some formulation, is in fact equal to $2 * v$ or the distance between the vertexes of each hydrophone's hyperbola. Therefore, it is possible to trace a hyperbole that represents the positions of the target in space both based on their distance and the signal's ToA. In the exceptional case where $d_3 = d_4$, we can observe that the possible positions are represented by an equidistant straight line to each hydrophone, such as the y axis.

4.2.1.4 ToA approximation

In order to estimate the location of an acoustic source we take into account the phase differences between each pair of hydrophones, carefully explained in section 4.1. These phase differences can be translated into periods of the signal which combined with the ToA obtained from correlation of arriving acoustic signals are equivalent to relative distances.

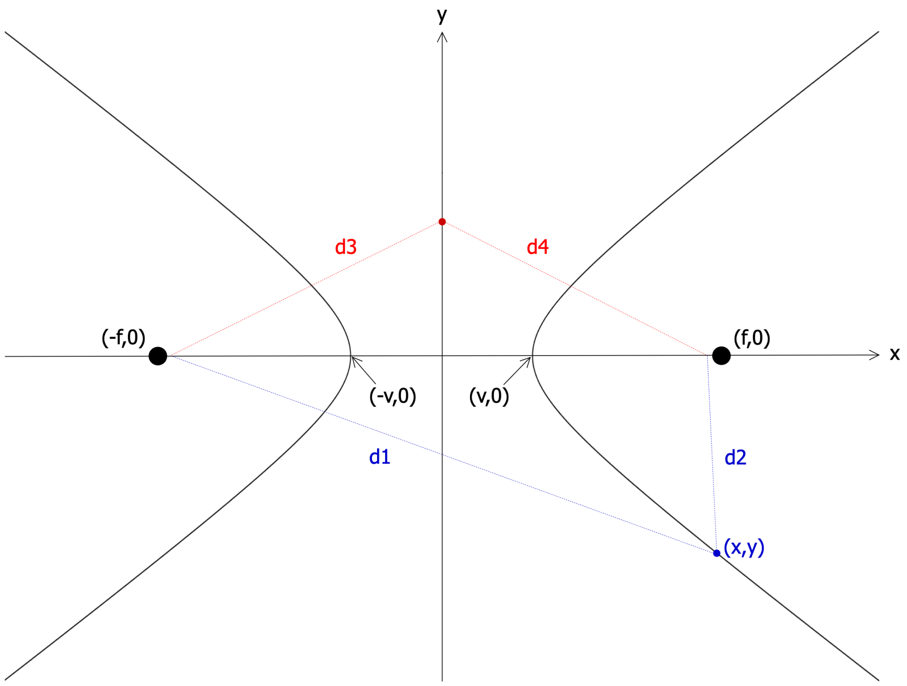

Figure 4.3: Hyperbolic representation of acoustic source position possibilities in relation to ToA to two hydrophones

Following the previous idea, it is possible to model the distance of one sensor to the target based on the known distance of a second sensor to the same target. This is to say that for two sensors with known relative positions where hydrophone 1 is the closer to the target, the distance from hydrophone i to the target, D_i, can be expressed as the distance of hydrophone j to the target, D_j, added by the time difference of arrival, Δt_{ij}, multiplied by the propagation velocity, c_s. Overall, this relationship is declared in equation 4.5.

$$D_i = D_j + \Delta t_{ij} * c_s \tag{4.5}$$

Therefore, the same logic can be applied for multiple hydrophones. In the present work, in which it is considered a system with four hydrophones, a synchronization mechanism allows to determine the signals' ToA between the transceiver and the hydrophones. However, in order to simplify the synchronicity and decrease errors that arise from it, the module that precisely computes the phase differences of the received signal in the hydrophones is used so that is possible to apply the relationship in 4.5. Consequently, a better angle of arrival estimation can be achieved when using this approximation than if all four times of arrival are used for the same purpose.

4.2.2 Methodological Approach

The goal of the proposed system is to estimate the position of an acoustic source in relation to known positions of a configuration of sensors, in a system of geometric axes with a defined origin.

For this purpose, the logic employed is based on vector algebra with other physical considerations, detailed in the present subsection.

Figure 4.4 represents the schematic of a considered scenario, where four hydrophones are placed in known relative positions in space and the origin of the axis is set on the body of the AUV or an alternative fixed structure. Then r_i is defined as the vector that connects the origin of the axis to hydrophone i and rr_i defines the vector that connects hydrophone i to the acoustic source. The black cross represents the acoustic source which is located somewhere in space. At last, the subtraction of the mentioned vectors is equal to r, according to 4.6, which corresponds to the position of the acoustic source in relation to the origin of the axis and, overall, it is the variable that the method aims to determine.

$$r_i = r + rr_i \tag{4.6}$$

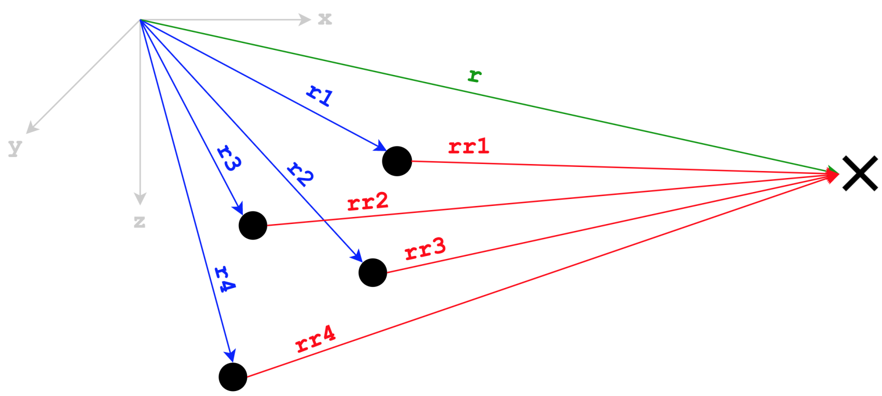

Figure 4.4: Considered scheme for angle of arrival estimation

Then we can define the times of arrival to each hydrophone as 4.7, where t_0 is the absolute time of emission, c_s is the underwater sound speed and ρ_i is the norm of rr_i, 4.11, which translates to the distance from hydrophone i to the acoustic source.

$$t_i = t_0 + \frac{\rho_i}{c_s} \tag{4.7}$$

However, as explained in the previous section, instead of using the absolute ToA in each hydrophone by computing the expression 4.7 for each of them, it can be expressed as a function of a single reference ToA. A simple logic was applied in order to determine this reference hydrophone, which starts by identifying the closest to the acoustic source. This allows to obtain all relative times of arrival by adding the defined reference time to each between a hydrophone and the reference one. This is achieved by analyzing the of each pair, Δt_{ij}, for all possible combinations of two among four hydrophones, making up a total of six combinations. Considering each hydrophone pair ij with $i, j = \{1,2,3,4\}$:

- if Δt_{ij} is positive, then hydrophone i is closer to the acoustic source
- if Δt_{ij} is negative, then hydrophone j is closer to the acoustic source
- if Δt_{ij} is zero, then i and j hydrophones are equidistant to the acoustic source

Considering these relations, it is possible to compose a vector that accumulates the closer hydrophone between each pair for a certain position of the acoustic source. Extracting the mode of this vector will then return the chosen hydrophone in most cases and therefore the overall closer to the acoustic source. If the closer hydrophones are the equidistant to the source, then it is indifferent which one is selected.

Thereafter, recalling expression 4.5, it is possible to write 4.8, 4.9 and 4.10 which translate the used relations, where the chose reference sensor is hydrophone 1, for the purpose of exemplification.

$$T_2 = T_1 + \Delta t_{12} * c_s \tag{4.8}$$
$$T_3 = T_1 + \Delta t_{13} * c_s \tag{4.9}$$
$$T_4 = T_1 + \Delta t_{14} * c_s \tag{4.10}$$

If then the distance ρ_i is raised to the power of two, we know that $||rr_i||^2 = r_i^T r_i$, which allows to deduce equation 4.12 after some mathematical manipulation. Considering ρ_i a physical distance, it is also possible to express it trough equation 4.13, which uses the speed of propagation underwater multiplied by the ToA of the signal from the acoustic source to hydrophone i.

$$\rho_i = ||rr_i|| \tag{4.11}$$
$$\rho_i^2 = r^T r + 2r^T r_i + r_i^T r_i \tag{4.12}$$
$$\rho_i^2 = c_s^2 (t_i - t_0)^2 \tag{4.13}$$

Since two distinct relations are defined for ρ_i^2, then it is possible to consider the algebraic expressions as equivalent, thus forming a single equation to be resolved with only one unknown variable. After some mathematical manipulation, the matrix relation 4.14 is achieved, where r is isolated and can be estimated.

$$\begin{bmatrix} 1 & 2r_i^T \end{bmatrix} \begin{bmatrix} r^T r \\ r \end{bmatrix} = \begin{bmatrix} c_s^2 (t_i - t_0) - r_i^T r_i \end{bmatrix} \tag{4.14}$$

In order to resolve this system of equations and isolate r, the least squares method is applied. If 4.14 is extended to the four considered hydrophones, we obtain matrix A represented as 4.15 and Y equivalent to 4.16. It is important to notice that the A matrix has to be invertible, thus the rows which contain the chosen hydrophone configuration have to be linearly independent. The least squares method is then expressed as 4.17, where X, $\mathbb{R}^4$, holds the Cartesian result of r. As the method formulates four equations that are meant to calculate only three coordinates, X will contain a fourth element that consists on a nonlinear component to $||r||^2$. This causes the estimator to be considered not efficient.

$$A = \begin{bmatrix} 1 & 2\,r_1^T \\ 1 & 2\,r_2^T \\ 1 & 2\,r_3^T \\ 1 & 2\,r_4^T \end{bmatrix} \tag{4.15}$$

$$Y = \begin{bmatrix} c_s^2\,(t_1 - t_0)^2 - r_1^T r_1 \\ c_s^2\,(t_2 - t_0)^2 - r_2^T r_2 \\ c_s^2\,(t_3 - t_0)^2 - r_3^T r_3 \\ c_s^2\,(t_4 - t_0)^2 - r_4^T r_4 \end{bmatrix} \tag{4.16}$$

$$X = (A^T * A)^{-1} * A^T * Y \tag{4.17}$$

After infer the Euclidean vector r, it is possible to obtain both the bearing trough its direction, $\hat{r}$, and the range through its magnitude, $||r||$.

4.2.3 Precision analysis

A methodology was formulated in order to evaluate the precision that the estimator can achieve in defined circumstances. For this initial approach to the study, the following conditions are considered:

a) **Sensor Configuration**

Each hydrophone configuration is analyzed individually. It is a parameter to be always defined and known from the begging of each simulation.

b) **Reference axis**

The origin of the reference axis is defined at the center of mass of the structure where the hydrophones are fixed, which in this case is the AUV.

c) **Injected error**

In order to make the study more realistic, an e_i error is added to the time differences of arrival, Δt_{ij}. These errors are mutually independent and follow a Gaussian distribution with zero mean and a configurable variance of σ^2, i.e., $e_i \sim \mathcal{N}(0, \sigma^2)$.

For the simulations performed in this project, a deviation of 5°,or a window of $[-2.5°, 2.5°]$, in the angle of arrival estimation was considered to be reasonable for an underwater navigation scenario. Therefore, since the specified period of the signal is $T = \frac{1}{24400}$ and one period corresponds to a 360° phase shift, then the 5° will be equivalent to $\frac{5°}{360°} * T$ which is approximately a deviation of $0.5\mu s$. Hence the considered standard deviation σ of the error e_i in the computed time differences of arrival is equal to $0.5\mu s$.

d) **Acoustic source position**

The considered positions for the acoustic source are defined in spherical coordinates. Thus the norm, n, corresponds to the source's range, whereas the azimuth, ϕ, and elevation, θ, define the angle of arrival of the received signal.

Recalling the definition of spherical coordinates, it is known that for elevations of -90° or 90°, the azimuth angle is meaningless and should not be considered. Since this system is affected by a Gaussian error, then the estimated azimuth angle is expected to return large errors not only for the absolute mentioned elevation values but for a considerable interval around it, dependent on the injected deviation. For that reason, the elevation values are limited to an interval between -80° and 80° so that the evaluated metrics present a result that is not so reflective of the errors originated from this phenomenon.

The positions to be estimated are contained in a matrix with a number of columns equal to the number of positions and three rows consisting of its spherical coordinates. The matrix is arranged so that for each defined norm, the elevation component covers the interval [-80° to 80°] in steps of one and, for each elevation value, the azimuth component covers the interval [-180°, 180°] in steps of one, forming partial spheres around the reference axis' origin.

e) **Propagation speed**

In all performed simulations, the considered speed of sound is 1500 m/s, which corresponds to the underwater propagation velocity of waves in typical conditions.

Having the conditions enumerated, the logic of the algorithm occurs as follows. For every defined position of the acoustic source, s, a function that consists on the estimator is called, receiving as input the s, the positions of the hydrophone configuration, r_i, and an injected error in the . It then returns the estimated position of the source in Cartesian coordinates, $[x, y, z]$, and in spherical coordinates, $[n, \phi, \theta]$. As the position s in Cartesian corresponds to the real value that is intended to be estimated, we can also obtain the real spherical coordinates by directly converting s using the Cartesian to spherical relations in 4.18.

$$\begin{cases} n = \sqrt{x^2 + y^2 + z^2} \\ \phi = arctan\frac{y}{x} \\ \theta = arctan\frac{\sqrt{x^2+y^2}}{z} \end{cases} \tag{4.18}$$

Consequently all conditions are met to analyze the achieved error in each coordinate by comparing the real position to the estimated values as 4.19, where the tested coordinates are x, y, z, n, ϕ and θ.

$$error_{coordinate} = |estimated_{coordinate} - real_{coordinate}| \tag{4.19}$$

The metrics used to evaluate the quality of the estimator were :

- **Mean squared error** (MSE): Incorporates both the variance and the bias of the estimator and indicates its overall quality
- **Standard deviation of the error** (σ) : Indicates how disperse are the estimates from the expected value
- **Minimum error** ($min(e_i)$) : Indicates the minimum error that is obtained by the estimator, thus the best absolute precision achieved

4.2.4 Simulations

A series of simulations were performed in order to understand the behavior and capabilities of the estimator and analyze its overall precision.

To illustrate a scenario where this estimator is applicable, we can consider that a vehicle is moving towards an acoustic signal transmitter whose position is unknown. Imagining that the target is at a considerable distance, then the main focus is to achieve an optimal bearing estimation which provides a more direct path and saves resources. The range estimation serves as secondary measurement that indicates how near the vehicle is from the destination, so that it is possible to make control decisions such as moderate the navigation speed in the proximity of the target. For the reasons outlined, the study that follows presents a more thorough analysis of the azimuth and elevation errors.

In this section, two different hydrophone configurations are considered, A and B defined in 4.1, where the columns r_{Ai} and r_{Bi} contain the position's coordinates of each hydrophones i.

	r_{A1}	r_{A2}	r_{A3}	r_{A4}	r_{B1}	r_{B2}	r_{B3}	r_{B4}
x	0.02	0.02	0	0	0.1	0	0	0
y	0	0	0.1	-0.1	0	0	-0.0707	0.0707
z	0.1	-0.1	0	0	0	0.1	-0.0707	-0.0707

Table 4.1: Hydrophone configurations for precision tests

For the first simulation, configuration A is tested for the acoustic source positions previously described, in a total of 58121. The obtained plots are illustrated in 4.5, where it is represented the error obtained by this specific configuration for all positions of the acoustic source.

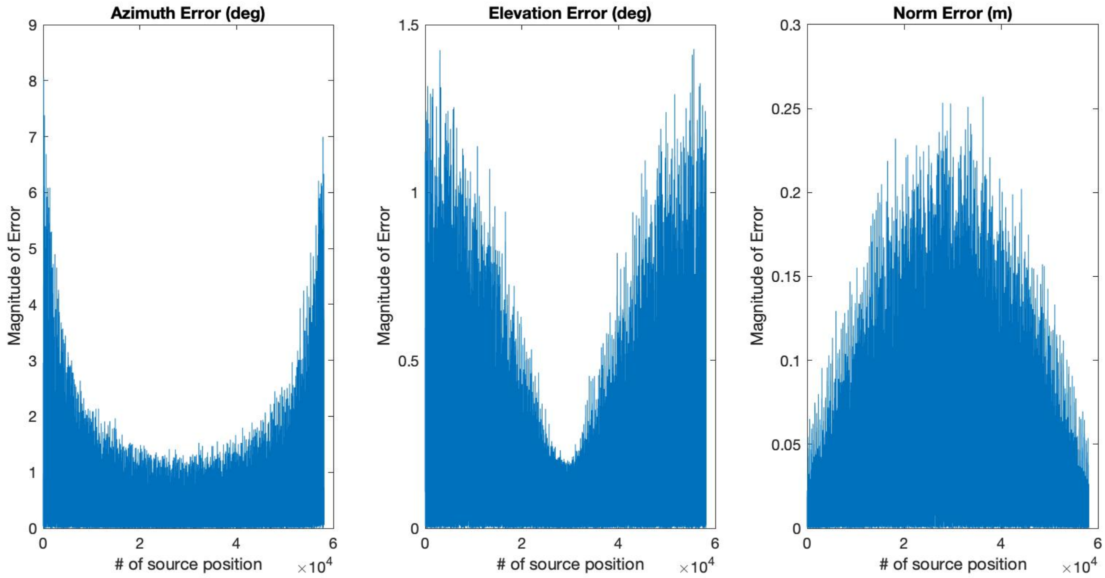

Figure 4.5: Plots of azimuth, elevation and norm errors for defined source positions

Some conclusions can be drawn about configuration A from the obtained results :

- A deviation in the estimate for positions with elevation close to its range limits causes:
  - a higher azimuth error, since
  - a higher elevation error, since the configuration has a shorter baseline along the xx axis, between the pairs of hydrophone that are aligned in the yy and zz axis, then the elevation is more precisely estimated in positions that are approximated perpendicular line that passes in the middle of the configuration.

-

Add all conclusions

Therefore, tables 4.2 and 4.3 illustrate the achieved results of azimuth error for several chosen norms.

Configuration	Norm	MSE	Standard Deviation	Minimum
A	10	0.5440	0.6050	8.7434×10^{-7}
	1000	0.5425	0.5992	8.3781×10^{-6}
B	10	0.2300	0.2129	1.3049×10^{-5}
	1000	0.2230	0.2115	4.0963×10^{-6}

Table 4.2: Comparison of obtained azimuth errors for different configurations

Configuration	Norm	MSE	Standard Deviation	Minimum
A	10	0.5440	0.1856	3.1025×10^{-6}
	1000	0.5425	0.1854	5.0595×10^{-6}
B	10	0.2300	0.0668	2.7903×10^{-5}
	1000	0.2230	0.0663	4.3935×10^{-6}

Table 4.3: Comparison of obtained elevation errors for different configurations

4.2.4.1 Influence of quantization on precision

The first term to be analyzed is how much does the quantization of the calculations influence the obtained precision of the estimator. In order to analyze this, a simple adaptation was made to the numeric precision of the values that are input of the system. Instead of using the MATLAB precision of fifteen decimal places, the value was truncated to a specified number of decimal places, κ. Since the time differences of arrival have magnitudes around microseconds, then initially the time differences of arrival are multiplied by 10^6 to avoid missing information. Then the relation 4.20 is applied resulting in a truncated value of with κ decimal places.

$$truncated = \frac{round(*2^{\kappa})}{2^{\kappa}}; \tag{4.20}$$

Finally after the truncation, the value is converted again to seconds to be used in the algorithm.

Dar um exemplo de erro antes e erro depois da truncação

4.2.4.2 Influence of ToA measurement on position estimation

por simulação, conclui que para distancias muito longe (quantizar) não faz diferença ter o TOA e basta os TDOA

4.2.4.3 Influence of displacing a specific hydrophone

The goal of this test is to understand what is the influence of moving one hydrophone along a certain direction in the overall error.

-considerar uma configuração
- analysar evolução do erro
-concluir que aumentar baseline é melhor até o erro manter-se constante

4.2.5 Conclusions

However there are conclusions that can be taken from the inspection of multiple configurations, such as :

- incresed baseline (até certo ponto) outputs best results ; when baseline for a specific hydrophone or pair is too large, then it will decrease the angle vision for the shorter baselines
- the higher the range, the bigger the errors
- in higher ranges, the small angle variations can still indicate a big deviation of estimation from the original point in Cartesian coordinates

- tenho sistema que estima os MSE, erro de azimute e elevação, para certas configuração consegue-se perceber padroes nos erros (e.g. erro aumenta com afastamento da source -> ao longe variações pequenas de angulo podem indicar deslocação da estimação grande)

escrever conclusoes gerais

Chapter 5

Dynamic reconfigurable configuration method

Having studied the estimator's behavior for several different configurations and conditions, there is still uncertainty about the best performance it can achieve. In the considered system, the hydrophone configuration has a decisive role on the achieved precision, as demonstrated. Therefore, a way to optimize the system's estimation would be to choose, for each position of the acoustic source, the configuration that returns the best estimation and thus the one that should be employed.

In a field scenario where a vehicle is searching for an acoustic transmitter, as it is navigating and readjusting its trajectory, the relative direction that is being estimated in real time is changing. Therefore, the system's performance can vary and arises the necessity of having different angles of vision from the hydrophones to the target. To resolve this issue, the proposed method assumes that the used USBL system integrates more than four hydrophones placed in known positions. This way, it is possible to dynamically reconfigure which four hydrophones are used at a time leading to an estimation that is optimal for the available sensors.

Another possibility is to determine through the same techniques which configuration of four hydrophones, tested in various positions along the vehicle, is the overall best for short and long range estimation. This can lead to a moderate compromise of the estimate precision, however decreases the number sensors that are employed and therefore the cost of the system.

This chapter is dedicated to explaining the methodological approach, the main findings and conclusions that were driven from the formulated dynamic reconfigurable configuration method.

descrever mais detalhadamente os temas que vao ser abordados no capitulo

- tendo em conta a posição do espaço, escolher a melhor configuração
- qual a melhor configuração (ou duas) para curto e longo alcance?
- tendo em conta a configuração qual é o local no espaço que consegue melhor resultados? (cramer rao)

5.1 Monte Carlo Approach

The developed algorithm serves as a tool to determine which is the best available hydrophone configuration for a certain target position. This approach uses a Monte Carlo method which is useful to solve problems that are deterministic in nature through repetition of and experiment with random parameter(s). Additionally,it makes use of the previously developed estimator, which is comprehensively explained in 4.2.2, to estimate the target position for each sensor configuration.

For this experiment, it is considered a total of nine hydrophones, whose positions are defined in table 5.1. Each column expresses the coordinates of each hydrophone, r_i, where the value of x_i is in the first row, the value of y_i in the second row and the value of z_i in the third row. Additionally, $q = 0.1$, $w = 0.1$ and $e = \frac{\sqrt{2}}{2} * w$.

	r1	r2	r3	r4	r5	r6	r7	r8	r9
x	q	0	0	0	0	0	0	0	0
y	0	0	0	w	-w	e	e	-e	-e
z	0	w	-w	0	0	e	-e	e	-e

Table 5.1: Position coordinates for an implementation with 9 hydrophones

These positions are arranged so that they can mimic a possible deployment in an AUV, as represented in figure 5.1, where hydrophone r_1 is placed in front of the vehicle and hydrophones r_2 to r_9 form a circle with a $10cm$ radius around the vehicle.

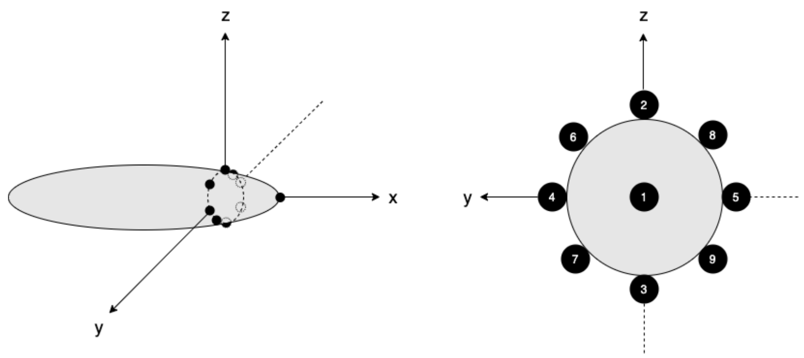

Figure 5.1: Hydrophone positions for an implementation with 9 hydrophones

Since the used configuration has to be three dimensional, it is defined that hydrophone r_1 always integrates the configuration as it is the only one in a different plan. Accordingly, the number of possibilities is combinations of three out of eight, $C(8,3)$, making up a total of 56 combinations.

Having the system presented, the algorithm will be explained next. For the sake of clarity, the algorithm was outlined in pseudo code and separated into two main parts, where 1 is integrated in 2.

verify all "line" and match with the algorithms

Algorithm 1 Determines the average azimuth errors, elevation errors and MSE for a set of hydrophone configurations

1: **for** `all k configurations` **do**
2:   **for** `all i estimation repetition` **do**
3:     $estimator(s, config(k), error)$ {returns estimate in Cartesian and spherical coordinates}
4:     `accum_estimate(i)` $\leftarrow$ `result of the estimator in each repetition`
5:     `accum_error_azimuth(i)` $\leftarrow$ `azimuth error in each repetition`
6:     `accum_error_elevation(i)` $\leftarrow$ `elevation error in each repetition`
7:   **end for**
8:   $mean\_estimate \leftarrow \frac{accum\_estimate}{accum\_samples}$
9:
10:   $deviation\_azimuth(config) = std(accum\_error\_azimuth);$
11:   $deviation\_elevation(config) = std(accum\_error\_elevation);$
12:   $error\_azimuth(config) = mean(accum\_error\_azimuth);$
13:   $error\_elevation(config) = mean(accum\_error\_elevation);$
14:
15:   $mse(config) = \sqrt{error\_azimuth(config)^2 + error\_elevation(config)^2};$
16: **end for**

Algorithm 1 is dedicated to computing the average azimuth error, elevation error and MSE for each of the $k = 56$ hydrophone configuration, in order to understand which of them achieves the minimum deviations when estimating a specific position. In order to do so, for each possible hydrophone configuration, the chosen acoustic source position s was estimated $i = 1000$ times (line 3), using the developed estimator, with an injected error to the TDoA that follows a Gaussian distribution with zero mean and a configurable variance of σ^2, i.e., $e_i \sim \mathcal{N}(0, \sigma^2)$. The result of this repetition would be an estimate cloud around the absolute s position, which indicates the estimation variation achieved by a certain configuration for a specific position in space. At each stage of the repetition, the estimate is accumulated and the errors of azimuth and elevation are calculated, similarly to the process described in the precision analysis 4.2.3 of the estimator. Therefore, after computing all estimation repetitions, it is possible to extract four essential parameters that define the quality of the estimation for each configuration:

- a mean estimate (line 8)
- the azimuth and elevation standard deviations (lines 10 and 11)
- the azimuth and elevation estimation errors (lines 12 and 13)
- the MSE (line 15)

Finally, using the obtained parameters it is already possible to determine three configurations that lead to the best estimation regarding MSE, azimuth deviation and elevation deviation. However, there are two main issues that this simple algorithm does not take into account:

1. For the considered system conditions, the error that is introduced is sufficient to originate different results every time the same position s is tested with the same injected error.

2. Assuming that the hydrophone system is deployed in an AUV, it is expected that every hydrophone has a blind spot which can correspond to the position that is being estimated. Regardless, a signal sent by an acoustic source in this situation can still be received by an hydrophone without line of sight to it, through reflections on path objects or reverberation in the surface of the AUV. Since these signals would be distorted and could lead to misinformation, they should not be considered. Consequently the hydrophones that do not have line of sight to the transmitter should be disregarded as well.

In order to resolve both these problems, a second part of logic was developed, which is translated in pseudo code 2.

In order to turn this mechanism more robust and solve the first issue, it is considered that the experiment of algorithm 1 has to be reiterated a defined number of times to obtain coherent and conclusive answers. Having said this, algorithm 2 begins with a loop that reiterates $j = 10$ times the logic previously explained. Addressing the second issue, the *line_of_sight* function (line 7) is called, serving as filter to determine which hydrophones do not have line of sight to the estimated position. The mathematical definitions included in this function are better clarified in the next subsection 5.1.1. Thereafter, all the configurations that have full line of sight to the transmitter are extracted. Meanwhile, the azimuth deviations, elevation deviations and MSE are accumulated in each experiment reiteration (line 8 to 10) so that it is possible to obtain the definitive mean of these parameters for each configuration (line 12 to 14). At this stage, it is possible to know already which are the configurations that are considered to achieve the minimum errors in each j reiteration and how many times each of them are chosen. However, these are still not filtered thus they can contain hydrophones that have not line of sight to the acoustic source. Next, only the configuration with full line of sight are extracted and three matrices are formed with the azimuth deviations, elevation deviations and MSE of these configurations. Having all the final parameters calculated and filtered, the overall best configurations for each of the chosen parameters are given by the minimum of the matrices that contain said parameter (line 17 to 19), i.e. for all configurations with full line of sight:

- The minimum obtained MSE corresponds to the configuration that more precisely estimates the position s in terms of MSE;
- The minimum obtained azimuth deviation corresponds to the configuration that more precisely estimates the position s in terms of azimuth;
- The minimum obtained elevation deviation corresponds to the configuration that more precisely estimates the position s in terms of elevation.

Additionally, it is possible to obtain the best configuration in terms of azimuth and elevation simultaneously, by computing the mean between the deviation of azimuth and elevation in each of the selected configurations. The minimum value obtained corresponds to the configuration which can decrease more the deviation in both parameters at the same time.

Algorithm 2 Determines the overall best configuration for a specific position estimation considering:
- multiple full experiments (Algorithm 1);
- only hydrophones with line of sight to the target.

for all j experiment reiterations **do**
    ****
    *** INSERT ALGORITHM 1 ***
    ****

    $line\_of\_sight(mean\_estimate, config)$ {returns which hydrophones have line of sight to the target}

    $reit\_mse = reit\_mse + mse$
    $reit\_dev\_azimuth = reit\_error\_azimuth + deviation\_azimuth$
    $reit\_dev\_elevation = reit\_error\_elevation + deviation\_elevation$
end for
$mean\_MSE = reit\_mse \div j$
$mean\_dev\_azimuth = reit\_dev\_azimuth \div j$
$mean\_dev\_elevation = reit\_dev\_elevation \div j$

Extract the configurations that contain only hydrophones with line of sight
Form matrix with errors of only the configurations with full line of slight

$[best\_config\_for\_mse,\ overall\_min\_mse] = min(overall\_mse)$
$[best\_config\_for\_azimuth,\ overall\_min\_dev\_azimuth] = min(overall\_dev\_azimuth)$
$[best\_config\_for\_elevation,\ overall\_min\_dev\_elevation] = min(overall\_dev\_elevation)$

5.1.1 Definition of line of sight

move this to appendix ?

As briefly explained before, when considering a set of hydrophones placed in the surface of an AUV, there will appear blind regions for each of the hydrophones. Since the transmitter can be positioned anywhere in space, it is essential to exclusively consider configurations whose hydrophones have line of sight, to avoid misinformation. In order to do to so, a region of space was defined for each hydrophone as the line of sight region, ls_i. As an illustrative example, if the acoustic source is placed outside the ls_4, the line of sight region of hydrophone r_4, then configurations containing r_4 should not be considered.

Two simplifications were initially considered: the AUV shape was approximated to geometric figures, composed by a cylinder as the body and a cone in the front; and the hydrophones were considered to be flat on the surface of the vehicle. Then, the line of sight regions are defined taking into account the tangential planes in the location of the hydrophone in every direction. Since hydrophone r_1 is always considered in every configuration, no line of sight region was defined for it.

explain this more decently

- $ls_2 \leftarrow$
- $ls_3 \leftarrow$

- $ls_4 \leftarrow$
- $ls_5 \leftarrow$
- $ls_6 \leftarrow$
- $ls_7 \leftarrow$
- $ls_8 \leftarrow$
- $ls_9 \leftarrow$

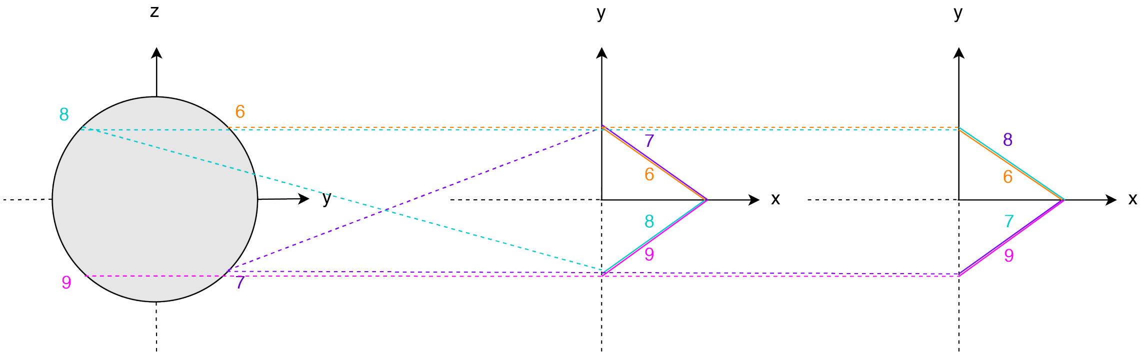

Figure 5.2: Projection of tangent to AUV's front for hydrophones 6, 7, 8 and 9

image of circle with hydrophones and regions of line of sight

5.1.2 Limitations of the system

5.1.3 Optimal solution based on range

If instead of wanting to determine in real time which four hydrophones should be used for the estimation we wanted to before hand know only one or two configurations that work acceptably well for short and long range, then we can do a monte carlo simulation to determine the best (or two) to employ from the beginning.

- Configurações com vista direta: seccionar campo de visão para cada hidrofone
- esta solução permite um ângulo de visão superior para posições no espaço do que outras soluções (literature review de valores tipicos)

5.2 Systematic comparison of geometric configurations performance

One of the aspects that can be studied to improve the localization estimation is analyzing the best sensor configuration that could be used for a certain scenario. Therefore, it was used the Crámer-Rao lower bound method to do a systematic study on the performance of several hydrophone configurations to be applied in many situations. The study serves as decision method for sensor configurations both applied in an AUV or in a situation without a vehicle.

The fundamental thought process and mathematical notation used in 2.7.1 are applied in the study that will be explained next.

5.2.1 Crámer-Rao bound

Following the logical approach for the process, there are three essential steps that can be differentiated:

1. Formulate the observations vector
2. Calculate the Fisher Information Matrix (FIM)
3. Calculate the determinant of FIM and draw conclusions

In this thesis, the number of used hydrophones per estimation is four, so all calculations will be presented for this specific case.

Firstly, the observations vector is formulated based on an initial time of arrival t_0, which is given by a synchrony mechanism integrated in the global communication system, and the time-of-arrival based on the vectors that connect the hydrophone positions, r_i, to the considered source, s_t. For a more realistic approach, it is also considered an added noise component that can be approximated to to a Gaussian distribution $n_i \sim \mathcal{N}(\mu, \sigma^2)$.

The four observations vector are then formulated as expressed in 5.5.

$$t_1 = t_0 + \frac{s_t - r_1}{c} + n_i \tag{5.1}$$

$$t_2 = t_0 + \frac{s_t - r_2}{c} + n_i \tag{5.2}$$

$$t_3 = t_0 + \frac{s_t - r_3}{c} + n_i \tag{5.3}$$

$$t_4 = t_0 + \frac{s_t - r_4}{c} + n_i \tag{5.4}$$

$$\tag{5.5}$$

Then, addressing the second step, all conditions are set to calculate the FIM, $I(d) \in \mathbb{R}^{3x3}$. In order to do so, if it is considered d$_i$ = $||s_t - r_i||$ as the distance between each sensor and the source, the gradient of the observations vector can be expressed as shown in 5.6.

$$\nabla_d t(d) = \frac{1}{c} \begin{bmatrix} \frac{d_1^T}{||d_1||} \\ \frac{d_2^T}{||d_2||} \\ \vdots \\ \frac{d_N^T}{||d_N||} \end{bmatrix} \tag{5.6}$$

Additionally, the added noise component which is introduces to the calculations is present in the covariance matrix used in the FIM equation, which is represented as in 5.7.

$$\Sigma = \begin{bmatrix} \sigma_1^2 & 0 & 0 & 0 \\ 0 & \sigma_2^2 & 0 & 0 \\ 0 & 0 & \sigma_3^2 & 0 \\ 0 & 0 & 0 & \sigma_4^2 \end{bmatrix} \tag{5.7}$$

Overall, the conditions to obtain the FIM matrix are established and, after some mathematical formulation, it is expressed as 5.8. This expression can be validated by a similar study made on TOA based optimal positioning [25].

$$I(d) = \frac{1}{c^2}\left[\sum_{n=1}^{N} \frac{d_i d_i^T}{||d_i||^2} \frac{1}{\sigma_i^2}\right] \tag{5.8}$$

The final step is to calculate the determinant and find its relation to the volume of the *uncertainty ellipsoid*. As mentioned before, in 2.7.1, the determinant of the Fisher Information matrix gives a deterministic value that represents the quantity of information that we can obtain and, therefore, the objective is to maximize it, by respecting the condition $argmax\, det(I(d))$, and consequently minimizing the volume of the ellipsoid.

5.2.1.1 Uncertainty Sphere

Firstly, it is necessary to choose a set of hydrophone configurations to be tested by the developed simulation environment. Therefore, considering the geometry of an AUV it was formulated a matrix containing nine hydrophones, from which are chosen four at a time to compose the configuration.

In order to evaluate the obtained determinant values, a way to give physical meaning to this result is to analyze it through the uncertainty volume. However, in an initial approach the ellipsoid was not considered and instead an uncertainty sphere was analyzed. The radius of the uncertainty sphere, *us*, is expressed as 5.9, which translates the three ellipsoid axis into a single mean radius that originates a figure of the same volume.

$$u_{sphere}(d) = \sqrt[2]{\sqrt[3]{det(I(d)^{-1})}} \tag{5.9}$$

By doing this, we know are looking to find the $argminur(d)$ which indicates that the error that originates that uncertainty radius is minimal.

5.2.1.2 Uncertainty Ellipsoid

eigenvalues give the length of each axis of ellipsoid

$$u_{ellipsoid}(d) = \sqrt[2]{eig(I(d)^{-1})} \tag{5.10}$$

5.2.2 Comparison with Monte Carlo simulation

All the concepts and notions before mentioned were applied in a simulated series of scenarios, where it is attempted to take conclusions about optimal positioning of the sensors for performance improvement. As such, the conditions of the simulation as well as the results of the study are hereinafter explained.

As mentioned before, the key to evaluate the performance when adopting this method is to analyze the determinant of the inverted FIM or, alternatively, the matrix's eigenvalues.

... Layout some results ...

Ideias:

1——

- tabela que para cada posição de 4 hidrofones, indica:
- raio de incerteza maximo e posição no espaço onde ocorreu
-raio de incerteza minimo e posição no espaço onde ocorreu
- desvio padrao de todos os pontos no espaço
- uncertainty ellipsoid

2——

plot do raio de incerteza para todas as posições no espaço de uma certa configuração

plot da nuvem de pontos e eigen vectors sobrepostos

comparar best configuration for short and long range

analyze plane wavefront solution for estimator somwhere

5.3 Conclusions

-planar wavefront is more simillar to cramer rao for long range source position estimation (discards the non linear components as cramer rao, has some limitations)

- cramer rao and monte carlo give different results because my estimator contains non linear components

Chapter 6

Conclusions

6.1 Summary

6.2 Contributions

The main contributions of this dissertation are:

- A HDL system design with strict area constraints that receives signals from four different sensors and calculates the phase differences between them
- An estimation algorithm for the angle of arrival of an acoustic signal to a configuration of four sensors
- An algorithm that chooses dynamically the best configuration of hydrophones, among a set of possible combinations, for a received signal with a certain angle of arrival

6.3 Future Work

The developed work arose various innovative ideas and topics according to the state of the art on localization optimization methods. Therefore, there is the intent to produce a a scientific article on the subject to be submitted in the OCEANS Conference 2021.

The adopted optimization techniques in the present work are the starting point of a topic which is not very explored in the current literature. Consequently, there are several areas that can be improved as follows:

- Implementing the developed algorithm for AoA estimation as a real-time system which can be used for decision making during underwater navigation
- Using Machine Learning techniques in order to find the optimal hydrophone array configuration, to be positioned in an underwater vehicle
- Integrating the estimator with a Kalman Filter or a Particle Swarm Optimization approach

References

[1] J. Liang, “Fifteen percent of ocean floor now mapped,” Jun 2019. [Online] Available: https://www.deeperblue.com/fifteen-percent-of-ocean-floor-now-mapped/. [Accessed Oct. 28, 2019].

[2] A. M. Bonito, “Acoustic system for ground truth underwater positioning in deec’s test tank,” Master’s thesis, Faculty of Engineering of the University of Porto, Porto, jul 2019.

[3] H. P. Tan, R. Diamant, W. K. G. Seah, and M. Waldmeyer, “A survey of techniques and challenges in underwater localization,” *Ocean Engineering*, vol. 38, no. 1, pp. 1663–1676, 2011.

[4] F. B. Jensen, W. A. Kuperman, M. B. Porter, and H. Schmidt, “Fundamentals of ocean acoustics,” in *Computational Ocean Acoustics*, pp. 3–17, Springer Science & Business Media, second ed., 2011.

[5] M. Stojanovic and J. Preisig, “Underwater acoustic communication channels: Propagation models and statistical characterization,” *IEEE Communications Magazine*, vol. 47, no. 1, pp. 84–89, 2009.

[6] J. M. F. M. aes, “Improving time of arrival estimation using encoded acoustic signals,” Master’s thesis, Faculty of Engineering of the University of Porto, Porto, jul 2018.

[7] D. E. Chaitanya, C. V. Sridevi, and G. S. B. Rao, “Path loss analysis of underwater communication systems,” in *IEEE Technology Students’ Symposium*, pp. 65–70, 2011.

[8] S. Gezici, “A survey on wireless position estimation,” *Wireless Personal Communications*, vol. 44, no. 3, p. 263–282, 2008. Springer Science & Business Media.

[9] B. M. R. Bharathi and A. R. Mohanty, “Underwater sound source localization by emd-based maximum likelihood method,” *Acoustics Australia*, vol. 46, no. 2, pp. 193–203, 2018.

[10] V. Chandrasekhar, W. K. Seah, Y. S. Choo, and H. V. Ee, “Localization in underwater sensor networks: survey and challenges,” in *WUWNet ’06: Proceedings of the 1st ACM international workshop on Underwater networks*, pp. 33–40, 2006.

[11] J. Esteves, A. Carvalho, and C. Couto, “Generalized geometric triangulation algorithm for mobile robot absolute self-localization,” in *2003 IEEE International Symposium on Industrial Electronics*, vol. 1, (Rio de Janeiro, Brazil), pp. 346–351, 2003.

[12] A. P. Pandian, T. Senjyu, S. M. S. Islam, and H. Wang, “Weighted trilateratiton and centroid combined indoor localization in wifi based sensor network,” in *Proceeding of the International Conference on Computer Networks, Big Data and IoT (ICCBI - 2018)*, pp. 163–166, jul 2019.

[13] M. Erol-Kantarci, H. T. Mouftah, and S. Oktug, "A survey of architectures and localization techniques for underwater acoustic sensor networks," *IEEE Communications Surveys & Tutorials*, vol. 13, no. 3, pp. 487–502, 2011.

[14] X. You, Y. Wu, M. Zhu, X. Li, and L. Zhang, "Low complexity short baseline localization algorithm based on taylor expansion," in *2019 IEEE International Conference on Signal Processing, Communications and Computing*, pp. 1–5, IEEE, 2019.

[15] K. G. Kebkala and A. I. Mashoshinc., "Auv acoustic positioning methods," *Gyroscopy and Navigation*, vol. 8, pp. 80–89, sep 2017.

[16] D. Sun, J. Ding, C. Zheng, and W. Huang, "An underwater acoustic positioning algorithm for compact arrays with arbitrary configuration," *IEEE Journal of Selected Topics in Signal Processing*, vol. 13, pp. 120–130, mar 2019.

[17] E. GmbH, "Underwater usbl positioning systems," 2018. [Online] Available: https://evologics.de/usbl. [Accessed Jan. 26, 2020].

[18] E. GmbH, "S2c technology," 2018. [Online]. Available: https://evologics.de/s2c-technology [Accessed Jan. 26, 2020].

[19] E. GmbH, "18/34 communication and positioning devices," 2018. [Online]. Available: https://evologics.de/acoustic-modem/18-34 [Accessed Jan. 26, 2020].

[20] E. GmbH, "S2c r 12/24 usbl communication and positioning device," 2018. [Online]. Available: https://evologics.de/acoustic-modem/12-24/usbl-serie [Accessed Jan. 26, 2020].

[21] Sonardyne, "Micro-ranger 2 shallow water usbl system," 2020. [Online]. Available: https://www.sonardyne.com/product/micro-ranger-2-shallow-water-usbl-system/ [Accessed Feb. 3, 2020].

[22] K. Maritime, "Hipap - high precision acoustic positioning," 2016. [Online]. Available: https://www.kongsberg.com/maritime/products/Acoustics-Positioning-and-Communication/acoustic-positioning-systems/hipap-models/ [Accessed May 2, 2020].

[23] A. N. Bishop, B. Fidan, B. D. O. Anderson, K. Doğançay, and P. N. Pathirana, "Optimality analysis of sensor-target localization geometries," *Automatica*, vol. 46, no. 3, pp. 479–492, 2010.

[24] E. Rady, M. M. E. A. El-Monsef, and M. M. Seyam, "Relationships among several optimality criteria," *Interstat*, vol. 15, no. 6, pp. 1–11, 2009.

[25] B. Ferreira, A. Matos, and N. Cruz, "Optimal positioning of autonomous marine vehicles for underwater acoustic source localization using toa measurements," in *2013 IEEE International Underwater Technology Symposium (UT)*, pp. 1–7, IEEE, 2013.